ISSN 1063-7850, Technical Physics Letters, 2020, Vol. 46, No. 7, pp. 665–668. © Pleiades Publishing, Ltd., 2020.
Russian Text © The Author(s), 2020, published in Pis'ma v Zhurnal Tekhnicheskoi Fiziki, 2020, Vol. 46, No. 13, pp. 43–46.

Spin Accumulation in the Fe_3Si/n-Si Epitaxial Structure and Related Electric Bias Effect

A. S. Tarasov[a,b]*, A. V. Luk'yanenko[a,b], I. A. Bondarev[a,b], I. A. Yakovlev[a], S. N. Varnakov[a], S. G. Ovchinnikov[a,b], and N. V. Volkov[a,b]

[a] *Kirensky Institute of Physics, Krasnoyarsk Scientific Center, Siberian Branch, Russian Academy of Sciences, Krasnoyarsk, 660036 Russia*

[b] *Institute of Engineering Physics and Radio Electronics, Siberian Federal University, Krasnoyarsk, 660041 Russia*

**e-mail: taras@iph.krasn.ru*

Received November 8, 2019; revised February 19, 2020; accepted April 6, 2020

Abstract—The electrical injection of the spin-polarized current into silicon in the Fe_3Si/n-Si epitaxial structure is demonstrated. The spin accumulation effect is examined by measuring the local and nonlocal voltage in a special four-terminal device. The observed effect of the electric bias on the spin signal is discussed and compared with the results obtained for ferromagnet/semiconductor structures.

Keywords: iron silicide, ferromagnet/semiconductor structures, Hanle effect, spin accumulation, electric spin injection.

DOI: 10.1134/S1063785020070135

The spin-dependent transport and magnetotransport in various nanostructures have been studied for several decades. The explosive development of this area started with the discovery of the giant magnetoresistance effect [1]. The design of a spin transistor proposed in [2] stimulated the creation of various spin devices [3]. In contrast to traditional electronics, which operates with the electron charge, spintronics uses the spin and spin current [4]. Silicon spintronics, which deals with the spin phenomena in silicon-based structures and devices, seems most promising. It offers the possibility of creating new spin-based devices using the highly developed silicon technology. Moreover, in the near future, this will allow the development of the hybrid devices that combine elements of both classical electronics and spintronics, as has already happened with magnetoresistive random access memory [5]. Silicon, along with good manufacturability, exhibits a weak spin–orbit coupling, which is necessary to implement spin transport at large distances. Therefore, silicon may become a basis for new-generation electronics, the main element of which is a spin-controlled field-effect transistor (SpinFET). The operation of a SpinFET and some other spin devices requires spin accumulation in nonmagnetic silicon, which needs to be somehow detected. The simplest and most electronics-friendly way to do this is by using electrical spin injection and detection [6]. To detect the spin accumulation effect, i.e., the nonequilibrium spin polarization induced by electrical injection, so-called "nonlocal spin transport measurements" (4T) [7] or the three-terminal Hanle method (3T) [8] are used. These approaches are widely used to study the features of spin transport in silicon structures, seek the most efficient injector materials, and improve the theory of spin diffusion [9, 10]. The search for optimal layer materials and composition and topology of various spin devices is being continued. This Letter explains the effect of spin accumulation and the impact of the electric bias on it in a device based on the Fe_3Si/n-Si epitaxial structure. The use of a light-doped ($n = 2 \times 10^{15}$ cm^{-3}) substrate for fabrication of the structure and the absence of a tunneling dielectric spacer in it did not prevent electrical spin injection into silicon.

A Fe_3Si ferromagnetic iron silicide film was formed on a phosphorus-doped n-Si(111) substrate with a resistivity of $\rho = 2\Omega$ cm ($n = 2 \times 10^{15}$ cm^{-3}) at 200°C using molecular beam epitaxy in ultrahigh vacuum. A growth chamber was equipped with a reflection high-energy electron diffraction (RHEED) system and an ellipsometer for in situ control of the growth process. The RHEED pattern obtained after the simultaneous deposition of Fe and Si is shown in Fig. 1a. One can see sharp reflections, which confirm that there has been successful epitaxial growth of the Fe_3Si film. Transmission electron microscopy and X-ray diffraction investigations confirmed that the film has a single-crystal structure.

A four-terminal (4T) planar device was fabricated in a process that included standard photolithography

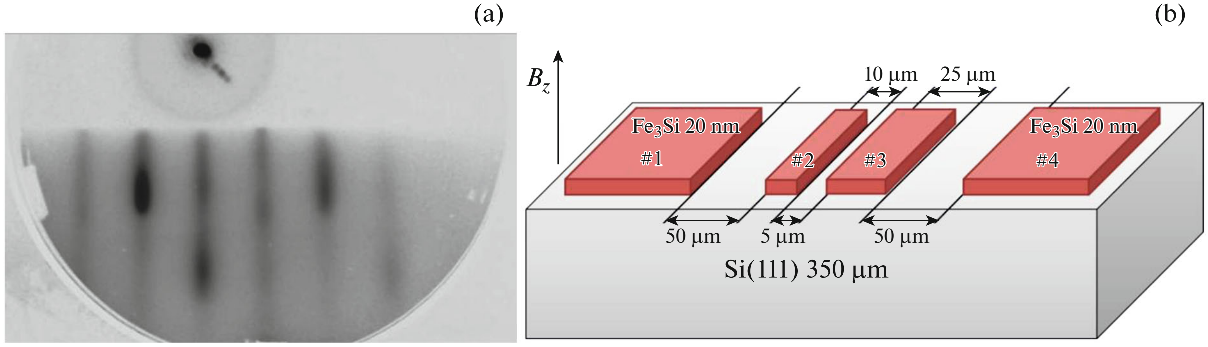

Fig. 1. (a) In situ RHEED pattern of the Fe_3Si film deposited onto the Si(111)7 × 7 surface at $T = 200°C$. Diffraction was obtained in the Si⟨101⟩ direction. (b) Schematic of a 4T device and the experimental geometry.

and wet chemical etching [11–13]. The Fe_3Si film was dissolved in an aqueous solution of hydrofluoric and nitric acids ($HF : HNO_3 : H_2O = 1 : 2 : 400$) at a room-temperature etching rate of 52 Å/s. After mask exposure, etching, and washing off, a device shown in Fig. 1b was obtained. The distance between nearest contacts 2 and 3 is 5 μm. To perform the electrical measurements, all the Fe_3Si contact pads were connected to the contact pads of the measuring cell by gold wires using a semiautomatic crystal-welding unit. The sample was then placed in a helium cryostat included in a measuring setup [14] equipped with an electromagnet and a Keithley 2634b measuring source. During the experiment, the temperature ranged from 4.2 to 300 K and the magnetic field was up to ±1 T.

First, we measured the I–V characteristics between all contacts (1, 2, 3, and 4), which were consistent with the temperature dependences of the resistance (Fig. 2a). The I–V characteristics for all the contacts are linear (see the inset in Fig. 2a) over the entire temperature range (from 4.2 to 295 K). Therefore, we can conclude that the Fe_3Si/n-Si contact is ohmic. This is confirmed also by the temperature dependence of the resistance recorded for contacts 2 and 3 (R_{23}), which shows a typical behavior for silicon. Surprisingly, this indicates the absence of a potential (Schottky or tunnel) barrier between Si and Fe_3Si. The ohmic contact between the metal and light-doped silicon can be formed due to the formation of an intermediate $Fe_{3-x}Si_{1+x}$ layer enriched with silicon at the initial film growth stage. Next, we measured the field dependences of local and nonlocal voltage ΔV at a bias current of $I = 100$ μA in the 3T and 4T experimental geometries (Figs. 2b, 2c). In both cases, the experimental curves are well approximated by the Lorentz function, which indicates spin accumulation in silicon [6]. The nonequilibrium spin lifetime can be calculated as

$$\tau_s = h/(2\pi g_e \mu_B \Delta B_z), \qquad (1)$$

where h is the Planck's constant, g_e is the Lande g factor ($g_e \approx 2$), μ_B is the Bohr magneton, and ΔB_z is the full width of the fitting curve at half maximum [12]. Analysis of the experimental data yields $\tau_s(3T) = 137$ ps and $\tau_s(4T) = 134$ ps for the 3T and 4T geometries, respectively. The calculated spin lifetimes are comparable with other data obtained for silicon-based structures. For example, in [15], it was reported that the lifetime in the Fe_3Si/n-Si structure with a silicon doping degree of 6×10^{17} cm^{-3} is 470 ps. In our previous study [13], we obtained $\tau_s = 145$ ps for the Fe_3Si/p-Si structure. In addition, it should be noted that, upon cooling down to 77 K, both spin signal ΔV and nonequilibrium spin lifetime τ_s monotonically increase and approximately double. This behavior is easy to understand if we assume that the main spin relaxation mechanisms are electron–phonon scattering and scattering by ionized dopant atoms, as was shown in theoretical work [16]. At the same time, it was experimentally demonstrated in [17] that, for n-Si, the temperature dependence of τ_s is caused by the temperature dependence of electron mobility μ_n and, consequently, diffusivity D_n, which are related by the Einstein equation $D_n = \mu_n(k_B T/q)$. Upon cooling, the number of events of scattering by both phonons and ionized atoms in our structure will decrease and the μ_n and D_n values will increase, which will eventually lead to an increase in τ_s.

Most interestingly, the dependence of the spin signal amplitude on the electric bias is observed. The measured 3T voltage ΔV_{23} increases with injected current I_{12}. However, the $\Delta V_{23}(I_{12})$ dependence is not quite linear. This can be clearly seen in Fig. 3, which shows the spin signal normalized to the current I_{12}. At the same time, recall that all the contacts of the device are ohmic (see the inset in Fig. 2a). Hence, the spin injection efficiency depends on the electric bias. At the same time, the calculated lifetime at different currents I_{12} varies, as expected, only within the error. In recent studies [9, 10] devoted to the structures based on heavily doped silicon ($n \sim 10^{18}$ cm^{-3}) and containing a tunneling MgO dielectric spacer, the effect of

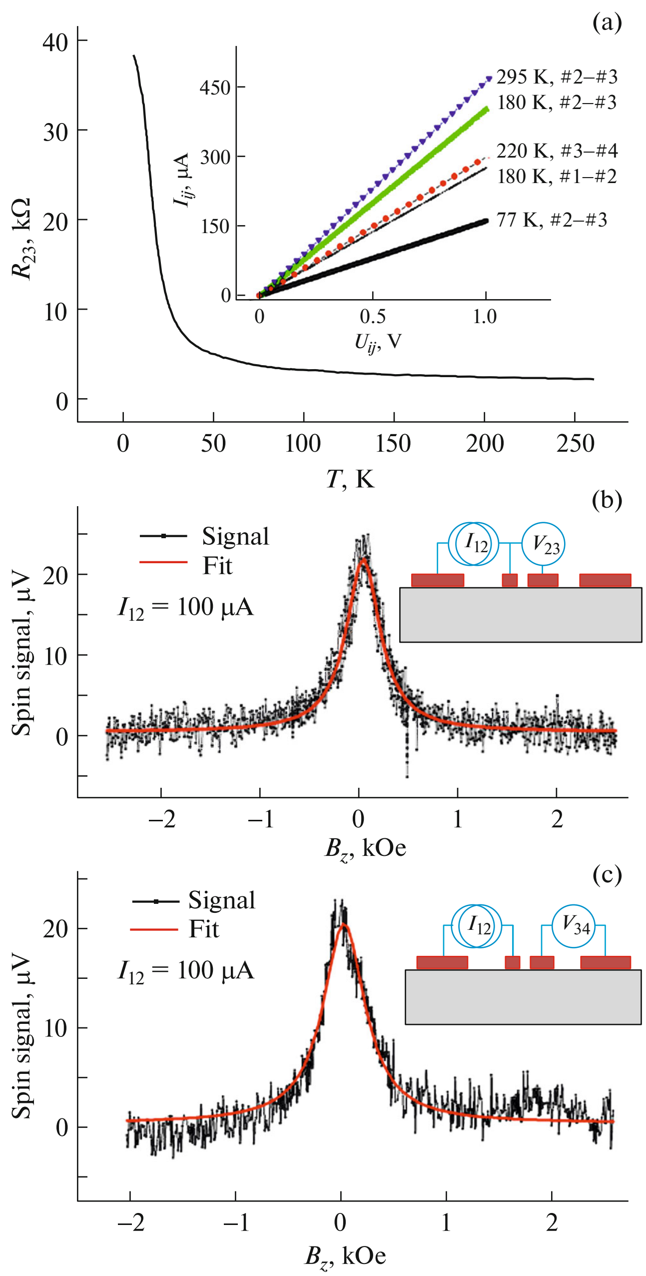

Fig. 2. (a) Temperature dependence of the resistance measured between contacts 2 and 3. Inset: *I*–*V* characteristics for different contacts at different temperatures. (b, c) Spin signal ΔV observed in the (b) three- and (c) four-terminal geometry at room temperature.

electric bias on different spin-dependent transport data was reported, including spin injection efficiency, spin polarization of the injected current, and 3T- and 4T-detected voltage ΔV. As in our case, there is a trend toward a decrease in the normalized spin signal and, consequently, the spin injection efficiency with increasing electric bias. We can suppose that this regularity is valid in a wide range of concentrations of nondegenerate silicon impurities (10^{15}–10^{18} cm^{-3}).

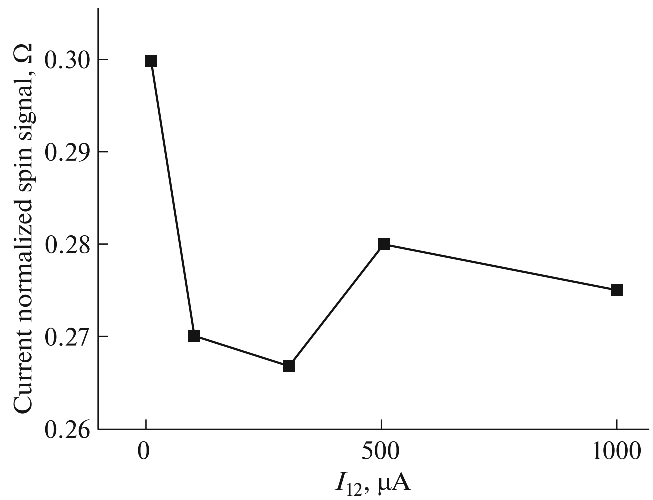

Fig. 3. Dependence of spin signal ΔV normalized to current I_{12} on current I_{12} in the 3T geometry.

However, further systematic investigations are required to fully understand the effect of electric bias and the drift charge current on the drift and diffusion spin current in silicon devices. We hope that our experimental results will help develop new ferromagnet/semiconductor devices based on spin-dependent transport phenomena.

FUNDING

This study was supported by the Russian Foundation for Basic Research, the Government of Krasnoyarsk krai, and the Krasnoyarsk Territorial Foundation for Support of Scientific and R&D Activities (project no. 18-42-243022), and a Grant of the Government of the Russian Federation for Creation of World Level Laboratories (agreement no. 075-15-2019-1886).

CONFLICT OF INTEREST

The authors declare that they have no conflict of interest.

REFERENCES

1. A. Fert, Rev. Mod. Phys. **80**, 1517 (2008).
2. S. Datta and B. Das, Appl. Phys. Lett. **56**, 665 (1990).
3. D. E. Nikonov and I. A. Young, Proc. IEEE **101**, 2498 (2013).
4. R. Jansen, Nat. Mater. **11**, 400 (2012).
5. L. Thomas, G. Jan, J. Zhu, H. Liu, Y. J. Lee, S. Le, R.-Y. Tong, K. Pi, Y.-J. Wang, D. Shen, R. He, J. Haq, J. Teng, V. Lam, K. Huang, T. Zhong, T. Torng, and P.-K. Wang, J. Appl. Phys. **115**, 172615 (2014).
6. A. Fert and H. Jaffres, Phys. Rev. B **64**, 184420 (2001).
7. X. Lou, C. Adelmann, S. A. Crooker, E. S. Garlid, J. Zhang, K. S. M. Reddy, S. D. Flexner, C. J. Palm-

stro[slash]m, and P. A. Crowell, Nat. Phys. **3**, 197 (2007).

8. R. Jansen, S. P. Dash, S. Sharma, and B. C. Min, Semicond. Sci. Technol. **27**, 083001 (2012).
9. S. Lee, F. Rortais, R. Ohshima, Y. Ando, S. Miwa, Y. Suzuki, H. Koike, and M. Shiraishi, Phys. Rev. B **99**, 064408 (2019).
10. A. Spiesser, Y. Fujita, H. Saito, S. Yamada, K. Hamaya, W. Mizubayashi, K. Endo, S. Yuasa, and R. Jansen, Phys. Rev. Appl. **11**, 044020 (2019).
11. A. S. Tarasov, A. V. Lukyanenko, I. A. Tarasov, I. A. Bondarev, T. E. Smolyarova, N. N. Kosyrev, V. A. Komarov, I. A. Yakovlev, M. N. Volochaev, L. A. Solovyov, A. A. Shemukhin, S. N. Varnakov, S. G. Ovchinnikov, G. S. Patrin, and N. V. Volkov, Thin Solid Films **642**, 20 (2017).
12. A. S. Tarasov, I. A. Bondarev, M. V. Rautskii, A. V. Lukyanenko, I. A. Tarasov, S. N. Varnakov, S. G. Ovchinnikov, and N. V. Volkov, J. Surf. Invest.: X-ray Synchrotr. Neutron Tech. **12**, 633 (2018).
13. A. S. Tarasov, A. V. Lukyanenko, M. V. Rautskii, I. A. Bondarev, D. A. Smolyakov, I. A. Tarasov, I. A. Yakovlev, S. N. Varnakov, S. G. Ovchinnikov, F. A. Baron, and N. V. Volkov, Semicond. Sci. Technol. **34**, 035024 (2019).
14. N. V. Volkov, A. S. Tarasov, D. A. Smolyakov, A. O. Gustaitsev, M. V. Rautskii, A. V. Lukyanenko, M. N. Volochaev, S. N. Varnakov, I. A. Yakovlev, and S. G. Ovchinnikov, AIP Adv. **7**, 015206 (2017).
15. Y. Fujita, S. Yamada, Y. Ando, K. Sawano, H. Itoh, M. Miyao, and K. Hamaya, J. Appl. Phys. **113**, 013916 (2013).
16. Y. Song, O. Chalaev, and H. Dery, Phys. Rev. Lett. **113**, 167201 (2014).
17. M. Ishikawa, T. Oka, Y. Fujita, H. Sugiyama, Y. Saito, and K. Hamaya, Phys. Rev. B **95**, 115302 (2017).

Translated by E. Bondareva